

1-1-1982

Characterization of shallow ion-implantations in VLSI devices with gated diode structures.

Chen-Chung Chao

Follow this and additional works at: <http://preserve.lehigh.edu/etd>

 Part of the [Electrical and Computer Engineering Commons](#)

Recommended Citation

Chao, Chen-Chung, "Characterization of shallow ion-implantations in VLSI devices with gated diode structures." (1982). *Theses and Dissertations*. Paper 2432.

This Thesis is brought to you for free and open access by Lehigh Preserve. It has been accepted for inclusion in Theses and Dissertations by an authorized administrator of Lehigh Preserve. For more information, please contact preserve@lehigh.edu.

CHARACTERIZATION OF SHALLOW ION-IMPLANTATIONS
IN VLSI DEVICES WITH GATED DIODE STRUCTURES

by

Chen-Chung Chao

A Thesis

Presented to the Graduate Committee

of Lehigh University

in Candidacy for the Degree of

Master of Science

in the Department of

Electrical and Computer Engineering

Lehigh University

December 1982

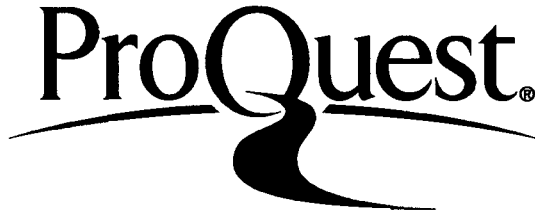
ProQuest Number: EP76708

All rights reserved

INFORMATION TO ALL USERS

The quality of this reproduction is dependent upon the quality of the copy submitted.

In the unlikely event that the author did not send a complete manuscript and there are missing pages, these will be noted. Also, if material had to be removed, a note will indicate the deletion.



ProQuest EP76708

Published by ProQuest LLC (2015). Copyright of the Dissertation is held by the Author.

All rights reserved.

This work is protected against unauthorized copying under Title 17, United States Code
Microform Edition © ProQuest LLC.

ProQuest LLC.
789 East Eisenhower Parkway
P.O. Box 1346
Ann Arbor, MI 48106 - 1346

This thesis is accepted and approved in partial
fulfillment of the requirements for the degree of
Master of Science.

December 8, 1982
Date

Professor in Charge

Chairman of Department

ACKNOWLEDGEMENTS

The author is deeply indebted to Dr. Marvin H. White for his constant guidance and encouragement throughout this work. Thanks are also due to Mr. A. K. Agarwal and Mr. F. M. Rhodes for their help in experimental setup and computer software development.

TABLE OF CONTENTS

	PAGE
Title Page	i
Certificate of Approval	ii
Acknowledgements	iii
Table of Contents	iv
List of Tables	v
List of Figures	vi
Abstract	1
Chapter	
1. Introduction	2
2. Theory	4
3. Experiment	10
4. Results and discussions	13
5. Conclusions	29
Appendix A	30
Appendix B	37
Appendix C	45
References	46
Vita	47

LIST OF TABLES

Table	Page
1. The parameters extracted from N-X curves by using non-linear least squares method.	25
2. The parameters extracted from N-X curves with corrections and from SUPREM.	27

LIST OF FIGURES

Figure	Page
1. MOS structure.	4
2. Cross-section of the gated diode structure.	10
3. Experimental setup and data acquisition system.	11
4. 10 KHz C-V curves with different V_{SB} .	13
5. Equivalent circuit of the gated diode in different regions.	14
6. N-X curves with $V_{SB} = -1$ V	16
7. N-X curves with $V_{SB} = -1.5$ V	17
8. N-X curves with $V_{SB} = -3$ V	18
9. N-X curves with $V_{SB} = -4$ V	19
10. N-X curves with different V_{sb} .	21
11. Curves before and after using non-linear least square method.	22
12. Curves before and after using Kennedy's correction.	23
13. Results from SUPREM	26
14. ω/λ and g_2 vs. g_1 , cf equation (A-27), (A-28) and (A-11).	36

ABSTRACT

The impurity profile, including the corrections near the semiconductor surface and junction, of a shallow ion-implanted layer has been characterized by C-V data obtained on a gated-diode structure with a microcomputer-controlled measurement system.

CHAPTER 1

INTRODUCTION

The knowledge of the doping profiles of a shallow ion-implanted layer is very important, especially in impurity profile related operating characteristics like the threshold voltage adjustment and punch-through control in VLSI device studies.

Traditionally, the doping profile has been obtained with the depletion approximation and C-V measurements; however, this is an approximation since the majority carriers distribution in the vicinity of the junction must be considered according to Kennedy and O'Brien [1]. In addition, the impurity profile near the semiconductor surface is influenced by accumulation of majority carriers as described by Ziegler, Klausmann, and Kar [2]. Brief reviews of the above theories will be given in chapter 2.

The microcomputer-based, automatic data-acquisition and analysis system will be outlined in chapter 3.

In chapter 4, the C-V curves and the corresponding equivalent circuit models of the various regions will be qualitatively described. The N-X curves of the shallow ion-implanted gated diode including the corrections near the semiconductor surface and near the junction will be discussed. The parameters like the the surface concentration, the peak concentration, the range of the ion implanation, the junction depth and substrate doping concentration extracted from the corrected N-X curves will be compared to the parameters from the Computer-Aided-Design program SUPREM.

The conclusions will be listed in chapter 5.

CHAPTER 2

THEORY

2.1 C-V profiling from Depletion Approximation

The differential capacitance in the depletion region of the C-V characteristics can be used to extract the impurity profile of the semiconductor devices. It can be derived as follows:

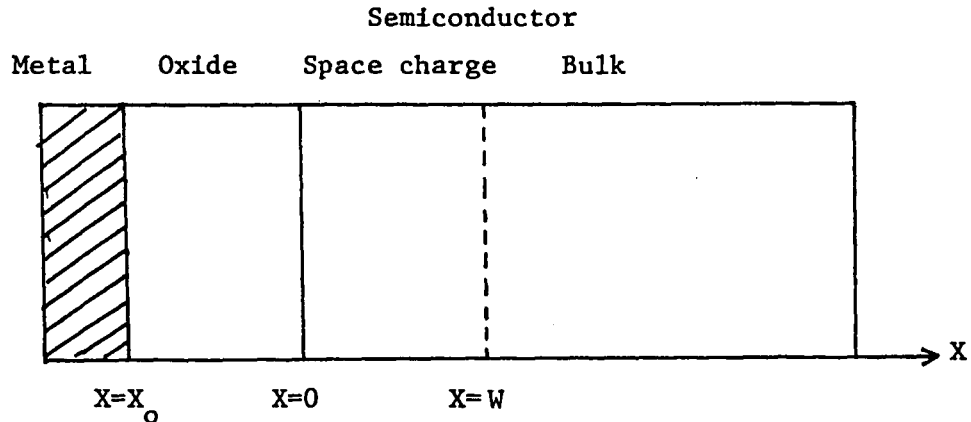


Figure 1. MOS structure

For an MOS structure in depletion shown in Figure 1., the gate charge dQ_G must equal the change in the space charge dQ_{SC} by Gauss' law, with the assumption of no net charge stored in the oxide. Thus

$$dQ_G = - dQ_{SC} \quad (2.1)$$

and
$$dQ_G = qN(W)dW \quad (2.2)$$

where dQ_{SC} space charge change is due entirely to the complete uncovering of additional ionized dopants, q is the charge of an electron, $N(W)$ is the dopant density (atoms/(cm**3)) at a distance W from the oxide-semiconductor interface.

$$dQ = C dV_{GB} \quad (2.3)$$

Equating (2.1) and (2.2), we obtain the variation of the gate-to-bulk voltage.

$$dV_{GB} = - qN(W) \frac{dW}{C} \quad (2.4)$$

where C represents the series sum of the oxide capacitance C_o and depletion capacitance C_{SC} .

$$\frac{1}{C} = \frac{1}{C_o} + \frac{1}{C_{SC}} \quad (2.5)$$

$C_o = \epsilon_o/X_o$ and $C_{SC} = \epsilon_s/W$, where ϵ_o the dielectric constant of the oxide, X_o the oxide thickness, ϵ_s the dielectric constant of the semiconductor and W the depletion width.

$$\text{Now} \quad dW = \epsilon_s d\left(\frac{1}{C_{SC}}\right) = \epsilon_s d\left(\frac{1}{C}\right) \quad (2.6)$$

So that

$$\begin{aligned} dV_{GB} &= -qN(W)\epsilon_s \left(\frac{1}{C}\right) d\left(\frac{1}{C}\right) \\ &= \frac{\epsilon_s qN(W)}{2} d\left(\frac{1}{C^2}\right) \end{aligned} \quad (2.7)$$

therefore,

$$N(W) = \frac{2}{\epsilon_s q} \left[\frac{d\left(\frac{1}{C^2}\right)}{dV_{GB}} \right]^{-1} = \frac{2C_o^2}{\epsilon_s q} \left[\frac{d\left(\frac{C_o}{C}\right)^2}{dV_{GB}} \right]^{-1} \quad (2.8)$$

From (2.5)

$$\begin{aligned} \frac{1}{C_{SC}} &= \frac{1}{C} - \frac{1}{C_o} = \frac{W}{\epsilon_s} \\ W &= \frac{\epsilon_s C_o}{C} \left(\frac{C_o}{C} - 1 \right) \\ &= \frac{\epsilon_s X_o}{\epsilon_o} \left(\frac{C_o}{C} - 1 \right) \end{aligned} \quad (2.3)$$

Equations (2.8) and (2.9) are the basis for the dopant determination from C-V measurement on an MOS structure.

2.2 Impurity profile correction near the junction

Kennedy et al. [1] found that the impurity profile inferred from the differential capacitance of the semiconductor junction is not that of the impurity atom distribution but, instead, that of the majority carrier distribution. So we can relate the apparent impurity profile (majority profile) and the true impurity distribution with the following analysis:

Assume the measured differential capacitance C of the test junction and the majority carrier distribution $n(X)$ in N-type semiconductor.

It is

$$n(X) = - \frac{2C_o^2}{\epsilon_s q} \left[\frac{d \left(\frac{C_o}{C} \right)^2}{dV_{GB}} \right]^{-1} \quad (2.10)$$

where X is the test junction space charge layer width at the applied

biasing voltage V_{GB} .

The electric current within this material due to both drift and diffusion of majority carriers is given by

$$J_n = q D_n \frac{dn}{dx} - q M_n n \frac{dx}{dx} \quad (2.11)$$

When $J_n = 0$, we have to maintain an electric field containing the local variations of electron density.

$$E(x) = - \frac{dx}{dx} = - \frac{kT}{q} \left(\frac{1}{n(X)} \frac{dn(X)}{dx} \right) \quad (2.12)$$

Assuming extrinsic semiconductor material (neglect the contribution from minority carrier density) ; we have from Poisson's equation.

$$\frac{d}{dx} = \frac{q}{\epsilon_s} [N(X) - n(X)] \quad (2.13)$$

where $N(X)$ is the impurity atom distribution.

By combining (2.12) and (2.13), we obtain

$$- \frac{kT}{q} \frac{d}{dx} \left(\frac{1}{n(X)} \frac{dn(X)}{dx} \right) = \frac{q}{\epsilon_s} [N(X) - n(X)] \quad (2.14)$$

and therefore

$$N(X) = n(X) - \left(\frac{kT}{q} \right) \left(\frac{\epsilon_s}{q} \right) \frac{d}{dx} \left[\frac{1}{n(X)} \frac{dn(X)}{dx} \right] \quad (2.15)$$

Equation (2.14) rigorously relates the desired impurity atom distribution $N(X)$ to the majority carrier distribution $n(X)$.

2.3 Impurity profile correction near the semiconductor surface

Equations (2.8) and (2.9) are based on the assumption that the charge in the space charge region is solely due to the ionized dopants. The depletion approximation is only valid for the depletion region where $W \geq 2\lambda$, W is measured from the semiconductor surface, and λ is the extrinsic Debye Length [3] given as

$$\lambda_D = \sqrt{\frac{2kT\epsilon_s}{q^2 N(W)}} \quad (2.16)$$

k is Boltzmann's constant, and T the absolute temperature.

Ziegler et al. [2] have developed a method to determine the doping profile of the semiconductor right up to the surface. The corrected doping density becomes

$$N(W) = \frac{2C_o^2}{q\epsilon_s} \left[\frac{d\left(\frac{C_o}{C}\right)^2}{dV_{GB}} \right]^{-1} g_2\left(\frac{W}{\lambda_D}\right) \quad (2.17)$$

$$W = \frac{sX_o}{\epsilon_o} \left(\frac{C_o}{C} - 1 \right) \left[1 - g\left(\frac{W}{\lambda_D}\right) \right] \quad (2.18)$$

where

$$g_2\left(\frac{W}{\lambda_D}\right) = \left(1 - \frac{2\left(\frac{W}{\lambda_D}\right)^2 g\left(\frac{W}{\lambda_D}\right)}{1 - g^2\left(\frac{W}{\lambda_D}\right)} \right) \frac{1}{1 - g\left(\frac{W}{\lambda_D}\right)} \quad (2.19)$$

$$\left(\frac{W}{\lambda_D}\right)^2 = g\left(\frac{W}{\lambda_D}\right) - \ln\left(g\left(\frac{W}{\lambda_D}\right)\right) - 1 \quad (2.20)$$

The procedures for calculating the doping profile is summarized as

follows:

1. Measure $g_1\left(\frac{W}{\lambda_D}\right)$ from C-V data

$$g_1\left(\frac{W}{\lambda_D}\right) = \frac{kT}{q} \frac{1}{C_o} \frac{d}{dV_{GB}} \left(\frac{C_o}{C}\right)^2 \quad (2.21)$$

$$= \frac{1 - g\left(\frac{W}{\lambda_D}\right)}{\left(\frac{W}{\lambda_D}\right)^2} \frac{2g\left(\frac{W}{\lambda_D}\right)}{1 - g\left(\frac{W}{\lambda_D}\right)} \quad (2.22)$$

2. Calculate $\frac{W}{\lambda_D}$ and g by solving equations (2.20) and (2.21)
3. Compute g_2 , where g_2 can be obtained from g_1 and g .

where

$$g_2\left(\frac{W}{\lambda_D}\right) = \frac{g_1}{2g + (1-g)g_1} \quad (2.23)$$

4. Finally, $N(W)$ and W are determined from equations (2.17) and (2.18)

$$N(W) = \frac{2C_o^2}{q\epsilon_s} \left[\frac{d\left(\frac{C_o}{C}\right)^2}{dV_{GB}} \right]^{-1} g_2\left(\frac{W}{\lambda_D}\right)$$

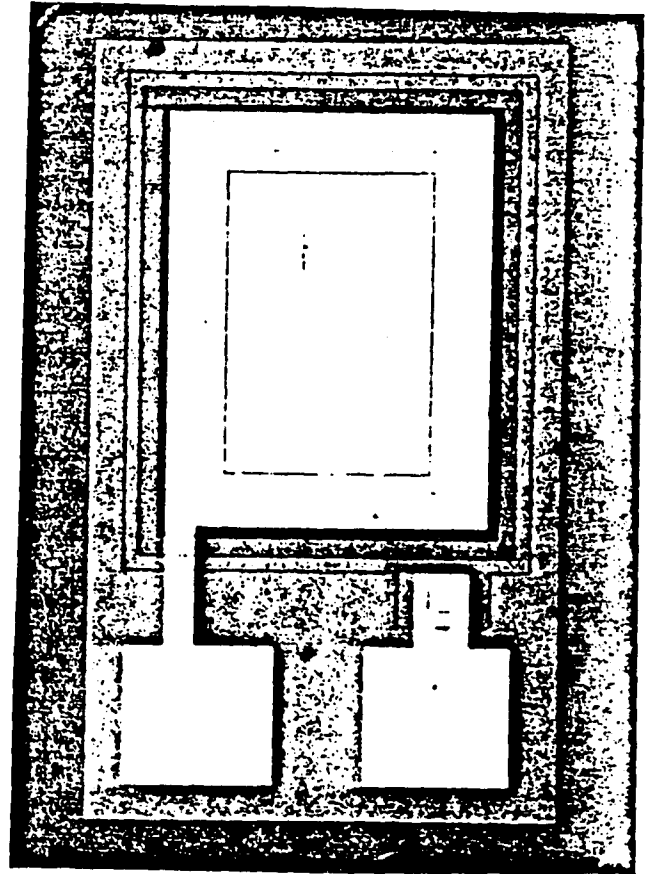
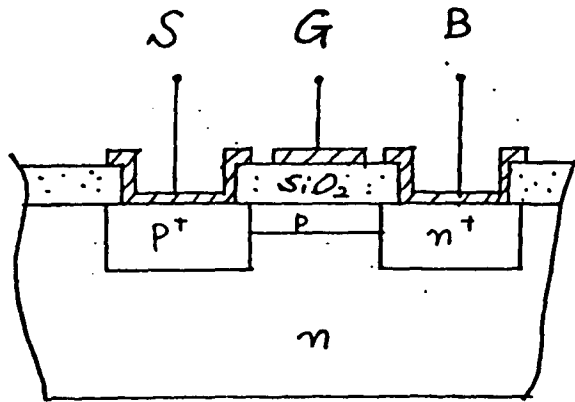
$$W = \frac{\epsilon_s X_o}{\epsilon_o} \left(\frac{C_o}{C} - 1 \right) \left[1 - g\left(\frac{W}{\lambda_D}\right) \right]$$

A detailed derivations of Ziegler's Theory will be shown in Appendix A.

CHAPTER 3

EXPERIMENT

The simplified cross section and photomicrograph of the gated diode structure is shown in Figure 2.



Simplified cross section

Photomicrograph

Figure 2. Cross-section of the gated diode structure

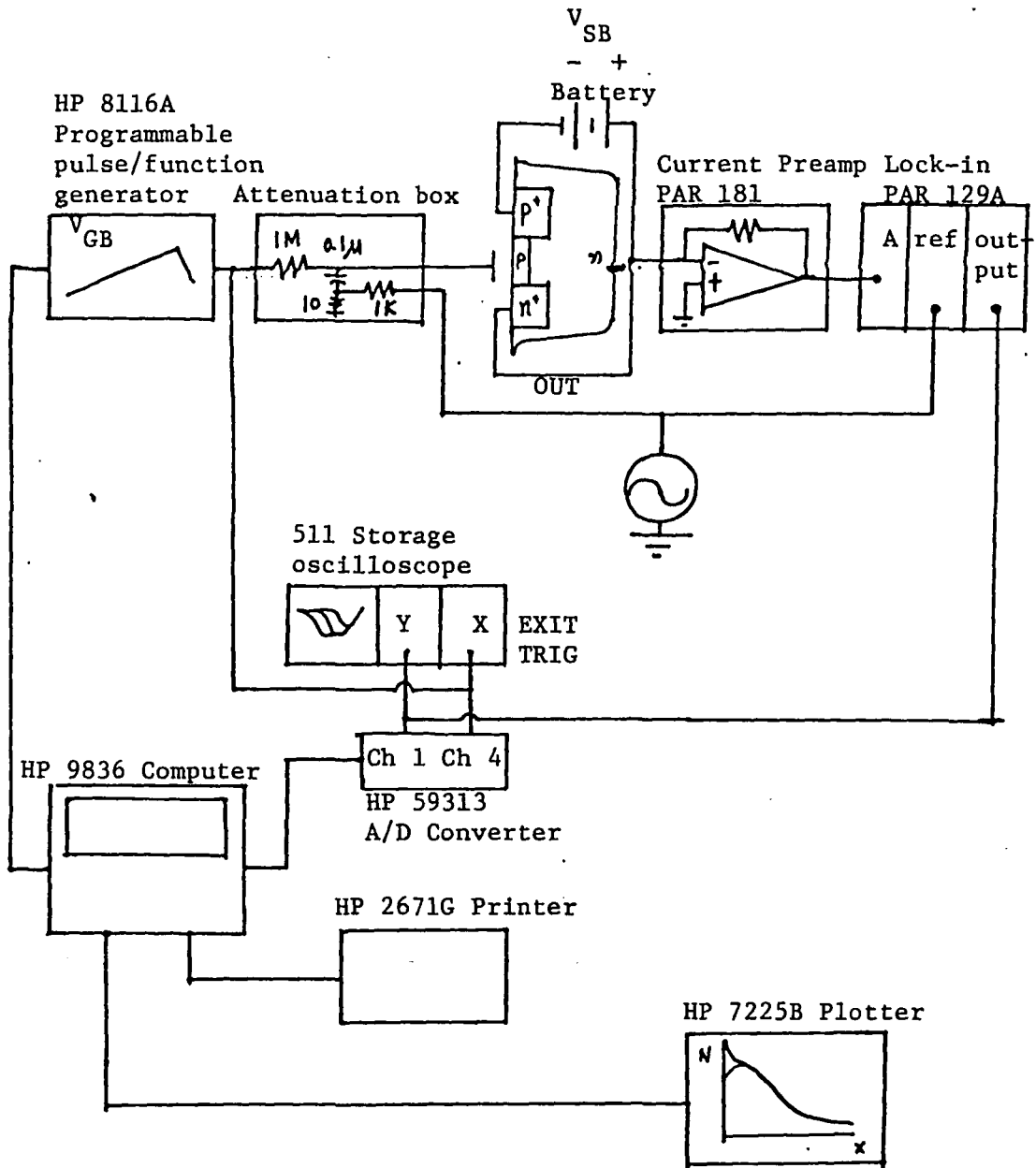


Figure 3. Experimental setup and data acquisition system.

Figure 3. is the experimental C-V setup and automatic measurement system diagram. The substrate of the gated diode (bulk) is connected to The inverting input of The current preamplifier. The gate terminal (gate) receives a ramped d-c voltage provided by HP 8116A programmable pulse/function generator and a small a-c signal. V_{SB} is supplied from battery in order to avoid the noise coming from the power lines. The output of the current preamplifier is proportional to the current through the gated diode, which consists of in-phase component due to conductance of the device and a quadrature-phase component due to capacitance. The output of quadrature-phase component of the lock-in amplifier is proportional to the capacitance of the gated diode. The bias voltage and the output of the lock-in amplifier can be applied to the horizontal and the vertical input of HP 511 storage oscilloscope (as a monitor device) and HP 59313 A/D converter (for data conversion use). A HP 9836 microcomputer is connected with a HP 59313 and a HP 8116A for instruments control, measurements, data collection and analysis.

All the computer programs developed for HP 9836 will be shown in Appendix B.

CHAPTER 4

RESULTS AND DISCUSSIONS

4.1 C-V curve

Figure 4 is a set of C-V plots of a buried channel p-channel gated diode with different V_{SB} .

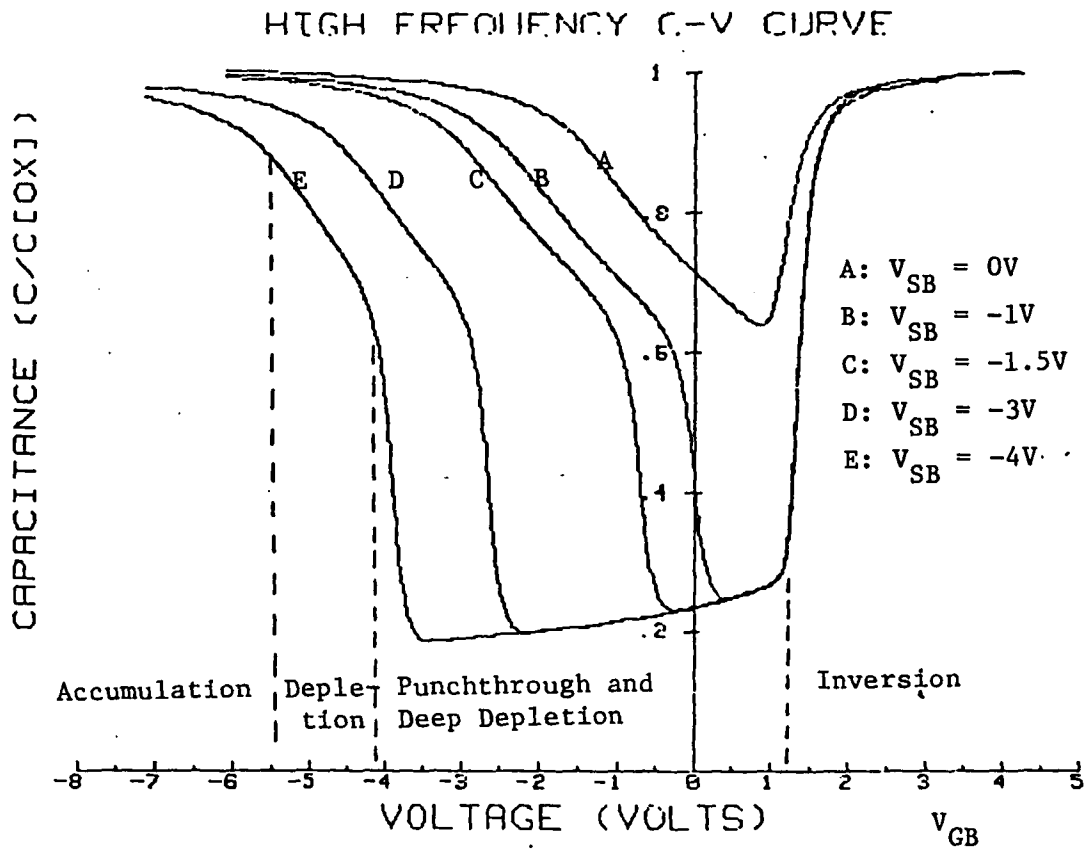
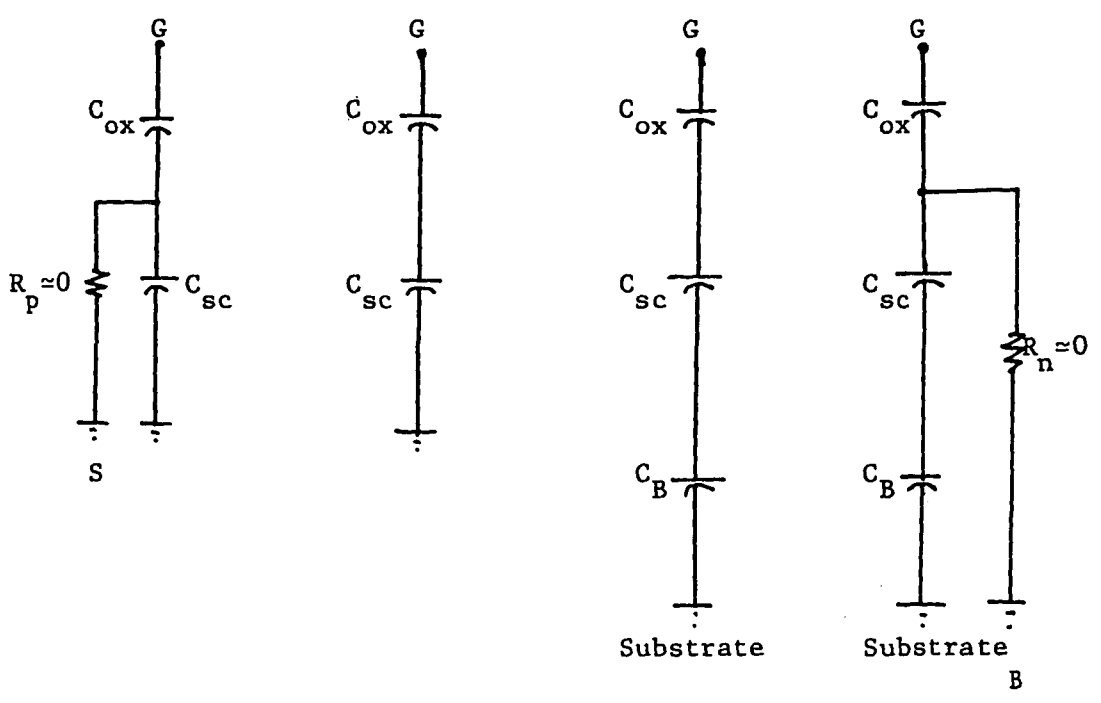
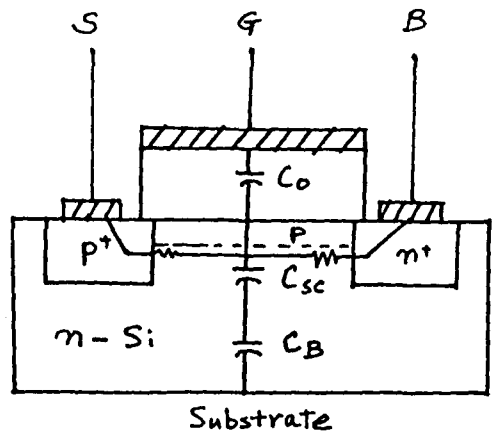


Figure 4. 10 KHz C-V curves with different V_{SB} .



Accumulation Depletion Punch-through and Deep Depletion Inversion

5A 5B 5C 5D

Figure 5. Equivalent circuit of the gated diode in different region.

A qualitative discussion of the various regions and the equivalent circuit model has been shown in Figure 5.

4.1.1 Accumulation [Figure 5A]

It can be characterized by the accumulation of majority carriers. There is a conductive path between the surface and the source (P+) . The equivalent capacitance is just the oxide capacitance.

4.1.2 Depletion [Figure 5B]

Holes are collected by P+ region and electrons are collected by the N+ region under this condition. There is no conductive path at surface either N+ or P+ regions, and the depleted P implant near the surface behaves as the space charge capacitance. The equivalent capacitance will be the series sum of the oxide capacitance and space charge capacitance.

4.1.3 Punch-through and Deep depletion [Figure 5C]

It can be characterized by complete depletion of the implant of all mobile carriers, leaving only space charge there, the depletion regions near the surface and the bulk p-n junction to be touched together. Besides the depletion capacitance and oxide capacitance, the bulk substrate capacitance has to be taken into account.

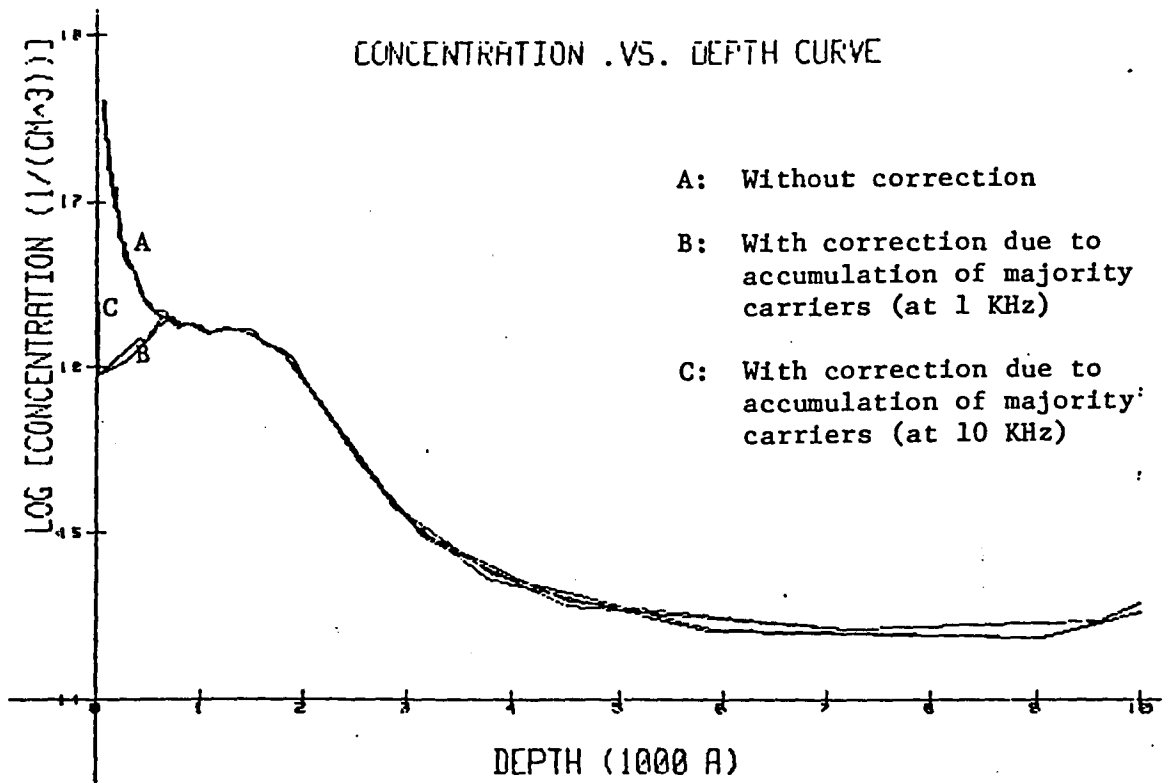


Figure 6. N-X curves with $V_{SB} = 1$ V.

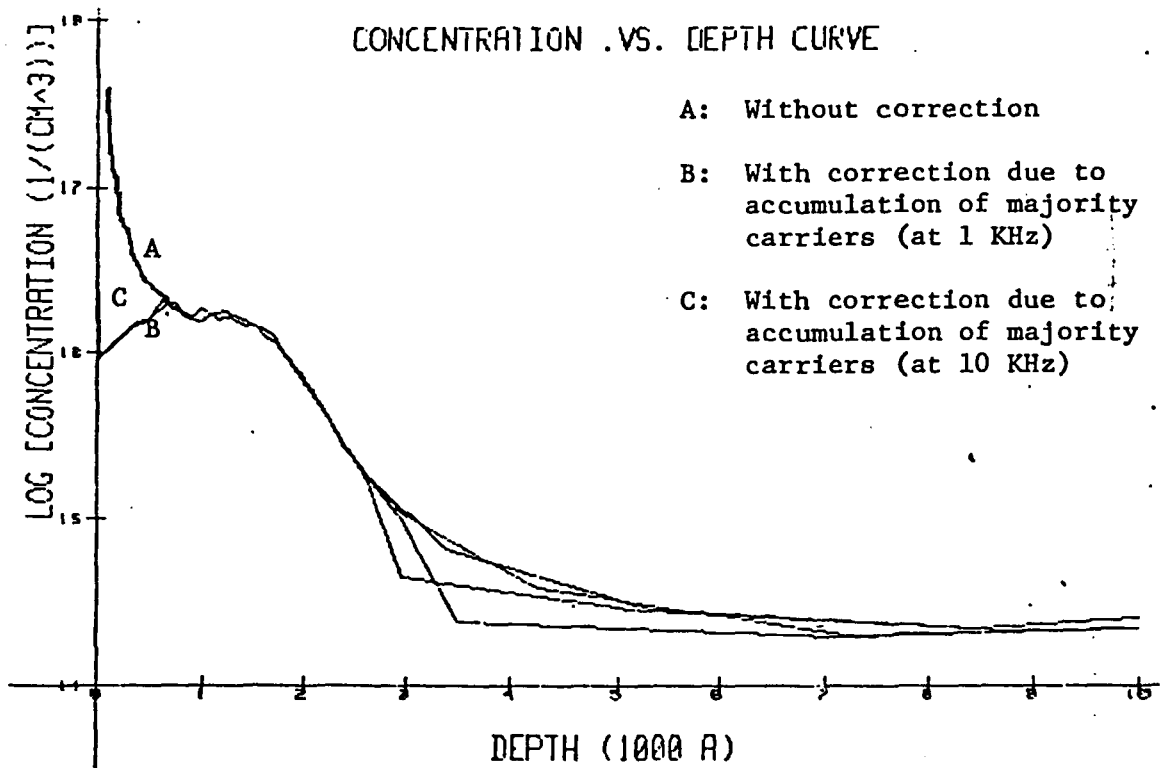


Figure 7. N-X curves with $V_{SB} = 1.5$ V.

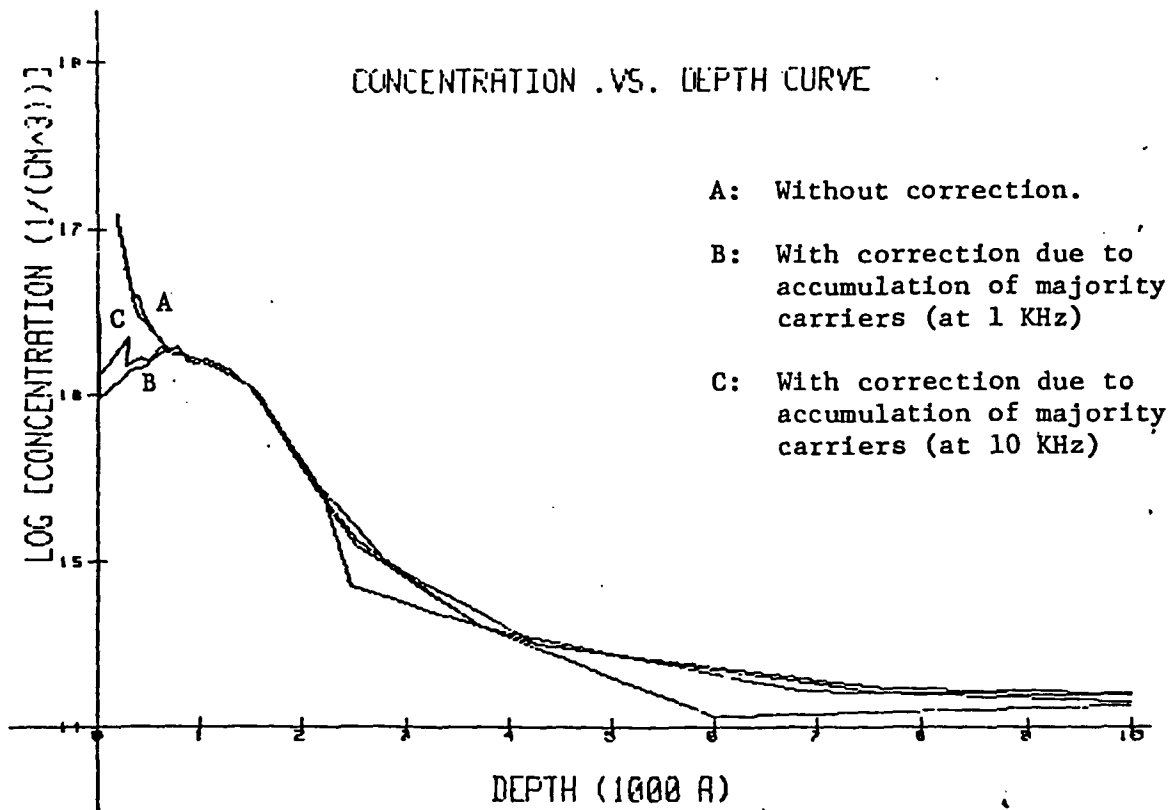


Figure 8. N-X curves with $V_{sb} = 3$ V.

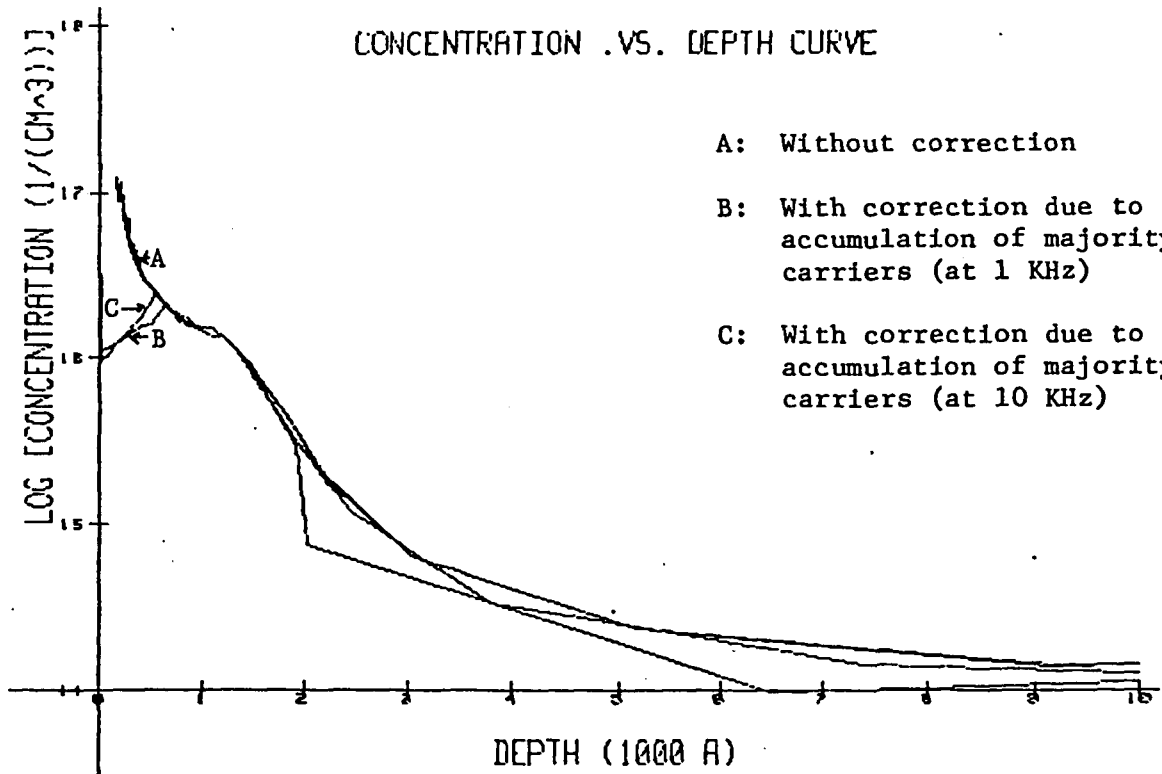


Figure 9. N-X curves with $V_{sb} = 4$ V.

4.1.4 Inversion [Figure 5D]

For enough positive voltage applied on the gate, electrons from the N^+ (bulk) will be attracted to the surface to invert it to N -type. This also produces a conductive path between the semiconductor and the N^+ region. Only the oxide capacitance contributes to the total capacitance.

4.2 N-X curve

By utilizing the equations (2.8) , (2.9) ,(2.17) , (2.18), the impurity profiles with and without correction near the semiconductor surface for various frequencies and source-to-bulk biases are shown from Figure 6 to Figure 9. For example, the impurity profile directly coming from C-V based on Depletion Approximation is shown in curve A of Figure 6. Curve B and curve C represent the impurity profiles obtained with correction near the semiconductor surface based on Ziegler's model at 1 KHz and 10 KHz, respectively.

From Figure 6 to Figure 9, In Figures 7, 8, and 9, there are clear deviations away from the uncorrected impurity profile around 3000 \AA . It is due to the effect of $W < 2\lambda$ and the nature of the correction performed with Ziegler's technique. Tracing back the Ziegler's theory, we have found it based on uniform doping assumption and extended to the slow-varying doping distribution. Thus, it is easily understood that such problems will take place in ion-implantation profiles near the junction. For Figure 10. different impurity profiles represent that the depletion widths are changing with different V_{SB} .

The non-linear least squares method has been employed to

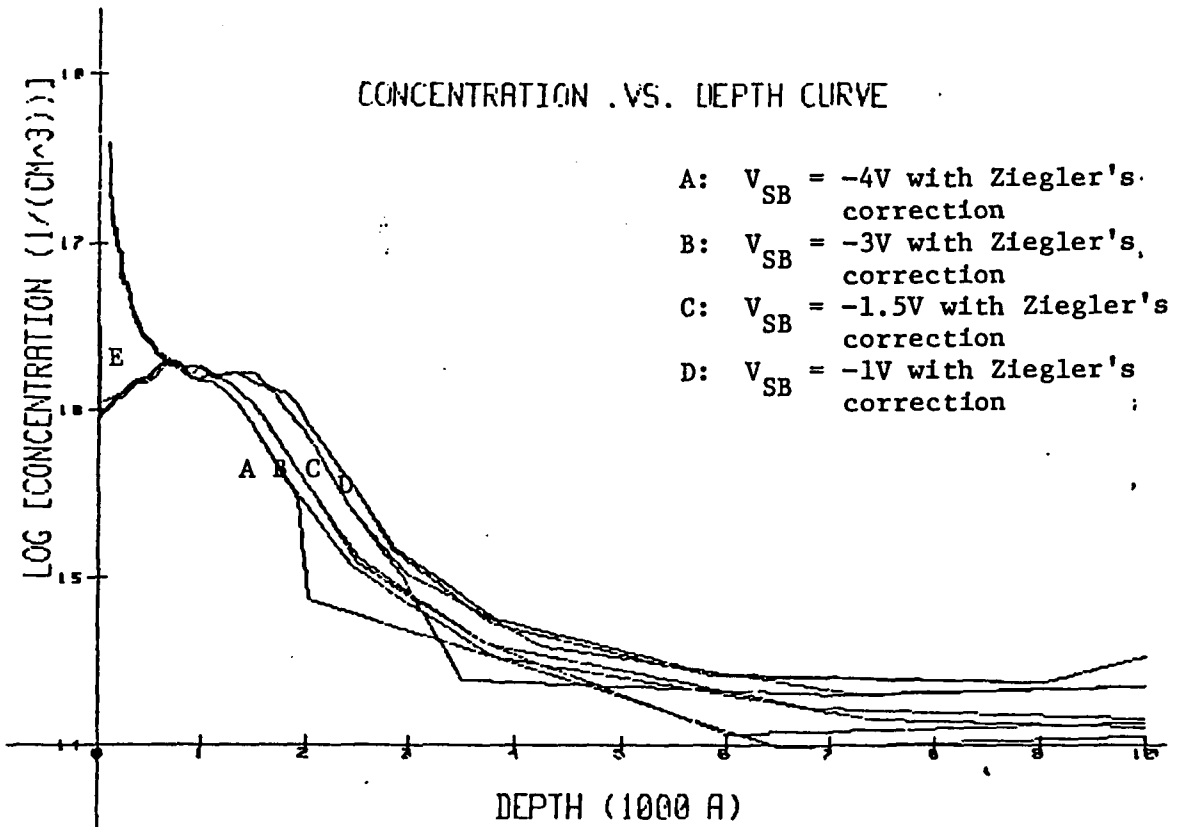


Figure 10. N-X curves with different V_{sb} .

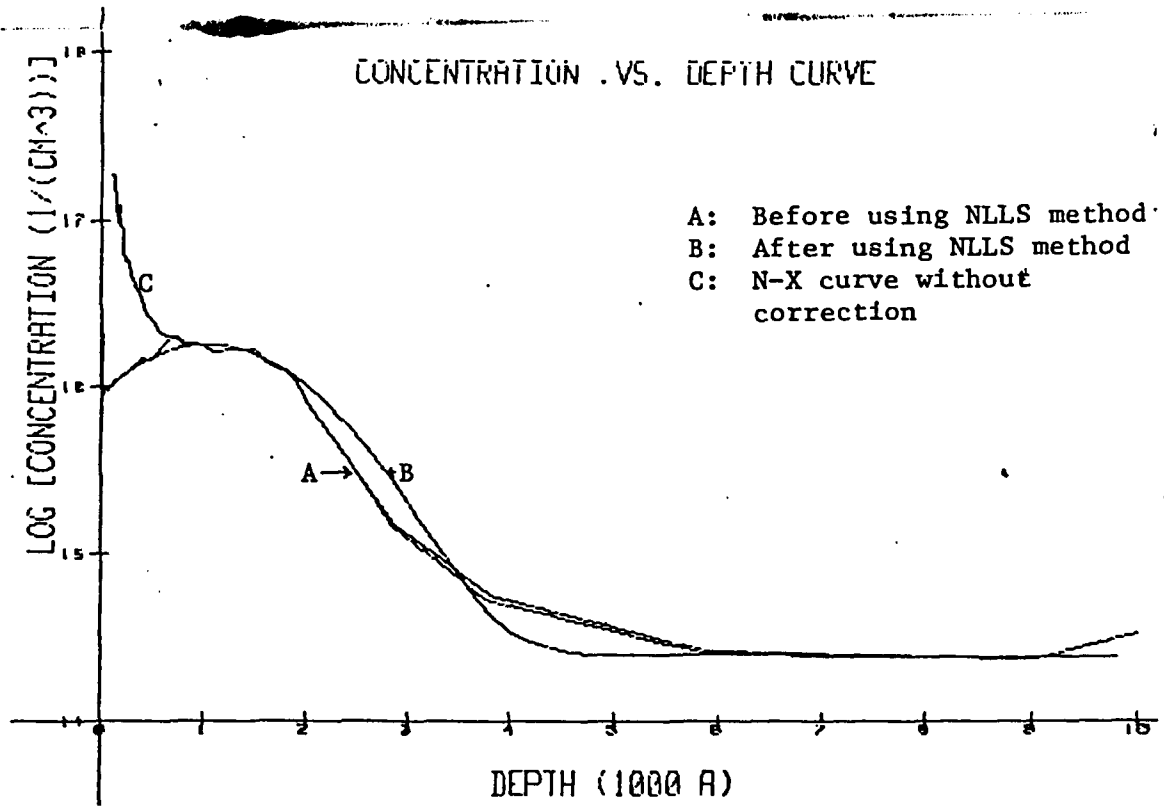


Figure 11. Curves before and after using non-least square method.

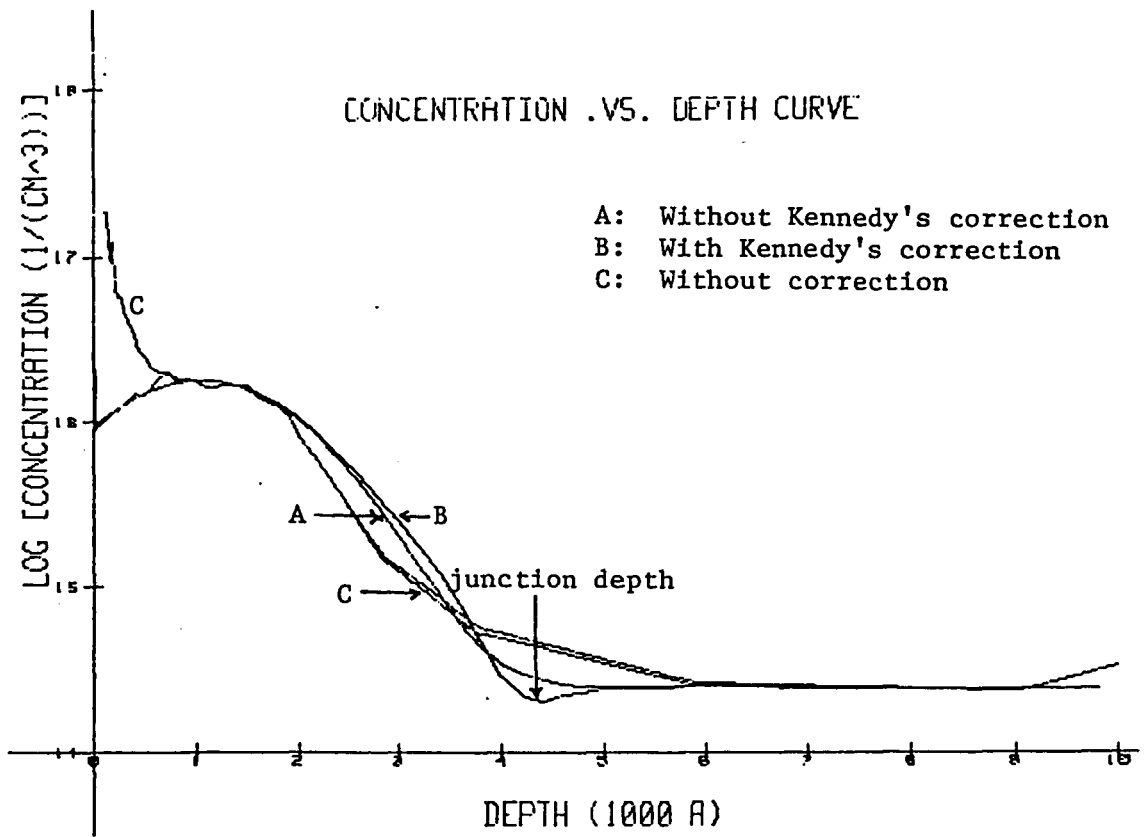


Figure 12. Curves before and after using Kennedy's correction.

extract parameters for ion-implantation profiles of the form

$$N(X) = N_0 e^{-\alpha(X-X_0)^2} + N_1 e^{-\beta X} - N_B \quad (4.1)$$

, where N_0 is the peak concentration, X_0 represents the range of the ion-implantation (R_p) and β is the channeling factor, N_B is the substrate doping.

The parameters with various biases has been listed on TABLE 1. Figure 11 shows the impurity profile before and after using non-linear least squares curve fitting technique. It clearly tells us that the peak concentration of the ion implantation can be accurately determined from this method within the tolerance of error [3]. It is still difficult to determine the substrate doping concentration from Figure 10, because the artificial tails obtained from C-V measurement is dependent on the biases V_{SB} [4]. The substrate doping determined from equation (4.1) from various N-X curves is around $2.E14 \text{ 1/(cm**3)}$.

Figure 12 shows the Kennedy's correction near the semiconductor junction by employing a non-linear least squares method to " curve fit ." We can roughly determine the junction depth by examining the N-X curve after correction.

TABLE 1. The parameters extracted from N-X by using non-linear least square method.

	NX1K10	NX10K10	NX1K15	NX10K15
N_0	1.80E16	1.78E16	1.79E16	1.76E16
α	66.83	71.27	69.47	69.68
X_0	0.1142	0.1137	0.1062	0.1036
N_1	4.5E14	4.7E14	4.0E14	4.5E14
β	0.01	0.01	0.01	0.01
N_B	2.E14	2.E14	2.E14	2.E14

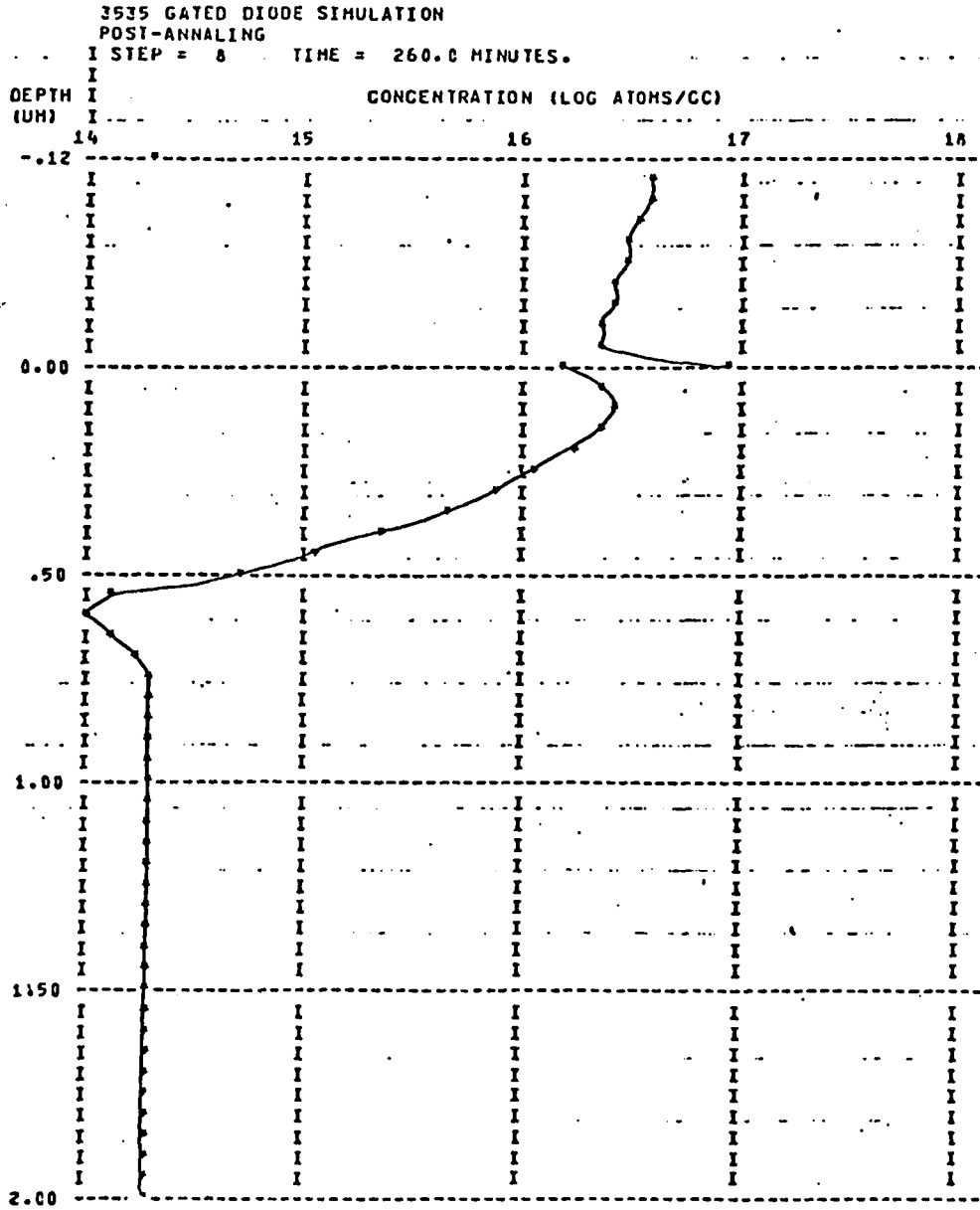


Figure 13. Results from SUPREM.

TABLE 2. The parameters extracted from N-X with corrections and from SUPREM.

	NX1K10	SUPREM	SUPREM
N_0	1.80E 16	2.33 E 16	2.51E 16
X_0	0.1142	0.1050	0.1050
N_B	2.E 14	2.E 15	2.E 14
N_s	0.99E 16	1.34 E 16	1.50E 16
X_j	0.4300	0.4206	0.5811

4.3 Simulation results from SUPREM

Now, we can compare the impurity profiles from C-V with corrections to the impurity profiles from SUPREM, which is a complete process simulation program for modeling semiconductor devices.

The fabrication sequences for the gated diode will be shown in Appendix C. The impurity profile from SUPREM will be shown in Figure 13.

From TABLE 2, which consists of the parameters extracted from SUPREM and parameters from the non-linear least squares technique, we conclude that the parameters like the surface concentration, the peak concentration, the range of the ion implantation, and the junction depth, can be determined within the tolerance of error from both sources.

CHAPTER 5

CONCLUSIONS

Summary of this thesis leads to the following conclusions:

1. A lot of time spent on the data collection and analysis has been saved after the establishment of an automatic data acquisition system and the development of the related parameters extraction computer software.

2. Some parameters extracted from corrected impurity profiles like the surface concentration, the peak concentration, the range of the ion implantation and the junction depth are comparable to the parameters obtained from SUPREM.

3. From the definition of the Debye Length, we understand it is a function of temperature. Thus, by decreasing the measurement temperature, we might obtain a more accurate doping profile close to the semiconductor surface.

4. A more accurate doping profile with taking the interface-state effects into account can be obtained from the comparison of the high-frequency and the low-frequency measurements [5].

Appendix A

The Derivations of Ziegler's Theory [2]

Since $C_{sc} = -\frac{dQ_{sc}}{d\psi_s} = -\left[\frac{dQ_{sc}}{dw}\right] \cdot \left[\frac{dw}{d\psi_s}\right]$, we shall first obtain $\frac{dQ_{sc}}{dw}$, and then $\frac{d\psi_s}{dw}$ in terms of $N(w)$ or w .

From the depletion approximation, w is the width of the depletion layer defined by the equation:

$$Q_{sc} = \int_0^{\infty} \rho_{sc}(x, w) dx = \pm q \int_0^w N(x) dx. \quad (A-1)$$

where Q_{sc} is the space charge per unit area, x the distance from the semiconductor surface, and $\rho_{sc}(x, w)$ the space charge density. (+ for n-type semiconductor and - for p-type).

Differentiation of equation (4) with respect to w leads to:

$$\frac{dQ_{sc}(w)}{dw} = \int_0^{\infty} \frac{\partial \rho_{sc}(x, w)}{\partial w} dx = \pm qN(w) \quad (A-2)$$

Here $N(w)$ means the doping density N at the distance $X = w$.

To obtain $\frac{d\psi_s}{dw}$, we begin with Poisson's equation

$$\frac{\partial^2 \psi(x, w)}{\partial x^2} = -\frac{\rho_{sc}(x, w)}{\epsilon_s} \quad (A-3)$$

Integrating (A-3) twice, we get

$$\psi_s(w) = -\frac{1}{\epsilon_s} \int_0^w \left\{ \int_0^x \rho_{sc}(x, w) dx \right\} dx$$

which when differentiated with respect to w gives

$$\frac{d\psi_s(w)}{dw} = - \frac{1}{\epsilon_s} \int_{-\infty}^0 \left\{ \int_{-\infty}^x \frac{\partial \rho_{sc}(x,w)}{\partial x} dx \right\} dx \quad (A-4)$$

Substitution of the integration variable x by x/λ and use the relation

$$\rho_{sc}(x,w) = q[N(x) - n(x,w)] \quad (A-5)$$

where $n(x,w)$ is the electron concentration, in equation (7) leads to:

$$\frac{d\psi_s(w)}{dw} = \frac{q\lambda^2}{\epsilon_s} \int_{-\infty}^0 \left\{ \int_{-\infty}^{x/\lambda} \frac{\partial n(x,w)}{\partial w} d\left(\frac{x}{\lambda}\right) \right\} d\left(\frac{x}{\lambda}\right) \quad (A-6)$$

First, we shall derive a relation for $\frac{\partial n(x,w)}{\partial w}$ in terms of N , w/λ and x/λ for uniform doping case.

For a constant doping density, equation (A-3) yields in case of $\psi_s \leq 0$, i.e. $Q_{sc} \geq 0$,

$$-\epsilon_x = \frac{\partial \psi}{\partial x} = \frac{2kT}{q\lambda} \left[\exp\left(\frac{q\psi}{kT}\right) - \frac{q\psi}{kT} - 1 \right]^{1/2} \quad (A-7)$$

Substitution of z into (A-7)

$$z = \frac{n}{n_0} = \exp\left(\frac{q\psi}{kT}\right) \quad (A-8)$$

and subsequent integration results in

$$\int_{\frac{n}{n_s}}^{\frac{n}{n_0}} \frac{dz}{z \sqrt{z - \ln z - 1}} = 2 \frac{x}{\lambda} \quad (A-9)$$

where n_0 is the electron concentration in bulk semi-

conductor and n_s is the electron concentration at semiconductor surface and

$$\lambda = \left(\frac{2kT\epsilon_s}{q^2 N} \right)^{\frac{1}{2}} \quad (\text{A-10})$$

From the relation $Q_{sc} = \epsilon_s \left(\frac{\partial \psi}{\partial x} \right) \Big|_{\psi=\psi_s}$ and $Q_{sc} = qNW$, cf. equations (A-1), (A-10), (A-7) and (A-8). We obtain the following relationship between W and n_s :

$$\begin{aligned} \frac{W}{\lambda} &= \left(\frac{n_s}{n_o} - \ln \frac{n_s}{n_o} - 1 \right)^{\frac{1}{2}} \\ &= (g - \ln g - 1)^{\frac{1}{2}} \end{aligned} \quad (\text{A-11})$$

where $\frac{n_s}{n_o}$ is limited to $0 \leq g \left(\frac{n_s}{n_o} \right) \leq 1$

To obtain $\frac{\partial n(x, w)}{\partial w}$, we start from Poisson's equation (A-3) and differentiate it with respect to w :

$$\begin{aligned} \frac{\partial^2}{\partial x^2} \left(\frac{\partial \psi}{\partial w} \right) &= - \frac{1}{\epsilon_s} \left(\frac{\partial \rho_{sc}}{\partial w} \right) \\ &= \frac{q}{\epsilon_s} \frac{\partial n}{\partial w} \end{aligned}$$

From equation (A-8), we have:

$$\frac{\partial \psi}{\partial w} = \frac{kT}{q} \frac{\left(\frac{\partial n}{\partial w} \right)}{n}$$

Then we obtain:

$$\frac{\partial^2}{\partial x^2} \left(\frac{\left(\frac{\partial n}{\partial w} \right)}{n} \right) = \frac{q^2}{kT\epsilon_s} \left(\frac{\partial n}{\partial w} \right) \quad (\text{A-12})$$

Since equation (A-12) is a self-adjoint differential

equation, it is clear that $y_1(x,w) = \frac{\partial n}{\partial x}(x,w)$ is one solution of equation (A-12). Assume the second solution of equation (A-12).

$$y_2(x,w) = y_1(x,w)U(x) \quad (A-13)$$

Substituting (A-13) into equation (A-12), we will obtain

$$U''(x) + \left\{ \frac{2n''}{n'} - \frac{2n'^2}{n} \right\} U'(x) = 0 \quad (A-14)$$

Assume $u'(x) = v(x)$, equations (A-14) becomes

$$v'(x) = \left\{ \frac{2n''}{n'} - \frac{2n'^2}{n} \right\} v(x) = 0 \quad (A-15)$$

The solution of (A-15) is $v(x) = \frac{n}{n'} = \frac{n}{\left(\frac{\partial n}{\partial x}\right)}$

$$\text{so } U(x) = \int_0^x v(x) dx = \int_0^x \frac{n}{\left(\frac{\partial n}{\partial x}\right)} dx$$

The general solution of equation (A-12) is

$$y(x) = C_1 y_1(x) + C_2 y_2(x)$$

Therefore

$$\frac{\partial n}{\partial w} = C_1 \frac{\partial n}{\partial x} + C_2 \frac{\partial n}{\partial x} \int_0^x \frac{n}{\left(\frac{\partial n}{\partial x}\right)} dx \quad (A-16)$$

Determination of C_1 and C_2 can be obtained from the following boundary conditions:

$$\lim_{n \rightarrow \infty} \frac{\partial n(x,w)}{\partial w} = 0 \quad (A-17)$$

$$\text{and } \int_0^\infty \frac{\partial n(x,w)}{\partial w} dx = n_0 \quad (A-18)$$

Using the relation $\frac{\partial n}{\partial x} = \frac{\partial n}{\partial \psi} \frac{\partial \psi}{\partial x}$ and equations (A-7) and (A-8), we obtain

$$\frac{\frac{\partial n(x, w)}{\partial x}}{\frac{n_0}{\lambda}} = 2 \frac{n}{n_0} \left(\frac{n}{n_0} - \ln \frac{n}{n_0} - 1 \right)^{\frac{1}{2}} \quad (\text{A-19})$$

Therefore, from equation (A-17), we find that $C_2 = 0$ and consequently $\frac{\partial n(x, w)}{\partial w}$ has the form of $C_1 \frac{\partial n(x, w)}{\partial x}$ only. From equation (A-18) and $N = n_0$, we finally get the solution:

$$\begin{aligned} \frac{\partial n(x, w)}{\partial w} &= \frac{N}{\lambda} f\left(\frac{x}{\lambda}, \frac{w}{\lambda}\right) \\ &= \frac{N}{\lambda} \left(- \frac{\frac{\partial n}{\partial x}}{1 - \frac{n_s \cdot n_0}{n_0 \cdot \lambda}} \right) \end{aligned} \quad (\text{A-20})$$

Equation (A-6) will become

$$\begin{aligned} \frac{d\psi_s(w)}{w} &= - \frac{qNW}{\epsilon_s} \frac{1}{1 - \left(\frac{n_s}{n_0}\right)} \\ &= - \frac{qNW}{\epsilon_s} \frac{1}{1 - g\left(\frac{w}{\lambda}\right)} \end{aligned} \quad (\text{A-21})$$

Let us now consider the non-uniform doping density $N(x)$.

$$\frac{\partial n(x, w)}{\partial w} = \frac{N(w)}{\lambda} f\left(\frac{x}{\lambda}, \frac{w}{\lambda}\right)$$

Substitution of the above equation in equation (A-6) and use of equation (A-21) result in:

$$\frac{d\psi_s}{dw} = - \frac{qN(w)}{\epsilon_s} \frac{w}{1 - g(\frac{w}{\lambda})} \quad (\text{A-22})$$

which when combined with equation (A-2) produce the desired relation for C_{sc} .

$$C_{sc} = \frac{\epsilon_s}{w} [1 - g(\frac{w}{\lambda})] \quad (\text{A-23})$$

Equations (A-11), (A-22) and (A-23) and the relation

$$\frac{d}{d\psi_s} \left(\frac{1}{C_{sc}^2} \right) = \frac{d}{dw} \left(\frac{1}{C_{sc}^2} \right) \frac{dw}{d\psi_s} \text{ lead to:}$$

$$\frac{d}{d\psi_s} \left(\frac{1}{C_{sc}^2} \right) = - \frac{1}{\epsilon_s q N(w)} \left\{ \frac{1}{1 - g(\frac{w}{\lambda})} - 2 \frac{w^2}{\lambda^2} \frac{g(\frac{w}{\lambda})}{[1 - g(\frac{w}{\lambda})]^3} \right\} \quad (\text{A-24})$$

from which, and equations (A-10) and (A-23), we finally obtain:

$$g_1 \left(\frac{w}{\lambda} \right) = \pm \frac{kT}{q_2} C_{sc}^2 \frac{d}{d\psi_s} \left(\frac{1}{C_{sc}^2} \right) \quad (\text{A-25})$$

$$N(w) = \pm \frac{2}{\epsilon_s q} \frac{d}{d\psi_s} \left(\frac{1}{C_{sc}^2} \right)^{-1} \cdot g_2 \left(\frac{w}{\lambda} \right) \quad (\text{A-26})$$

The functions g_1 and g_2 are given by

$$g_1 \left(\frac{w}{\lambda} \right) = - \frac{2g(\frac{w}{\lambda})}{1 - g(\frac{w}{\lambda})} + \frac{1 - g(\frac{w}{\lambda})}{\frac{w^2}{\lambda^2}} \quad (\text{A-27})$$

$$g_2 \left(\frac{w}{\lambda} \right) = \frac{1}{1 - g(\frac{w}{\lambda})} \left\{ 1 - 2 \frac{w^2}{\lambda^2} \frac{g(\frac{w}{\lambda})}{(1 - g(\frac{w}{\lambda}))^3} \right\} \quad (\text{A-28})$$

Graphs of g_2 vs g_1 and w/λ vs g_1 will be shown in Figure 14.

Determination of the semiconductor doping profile

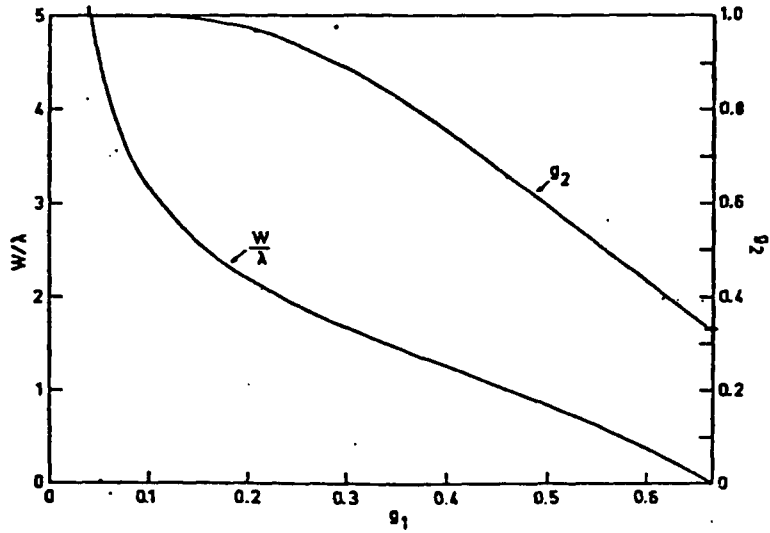
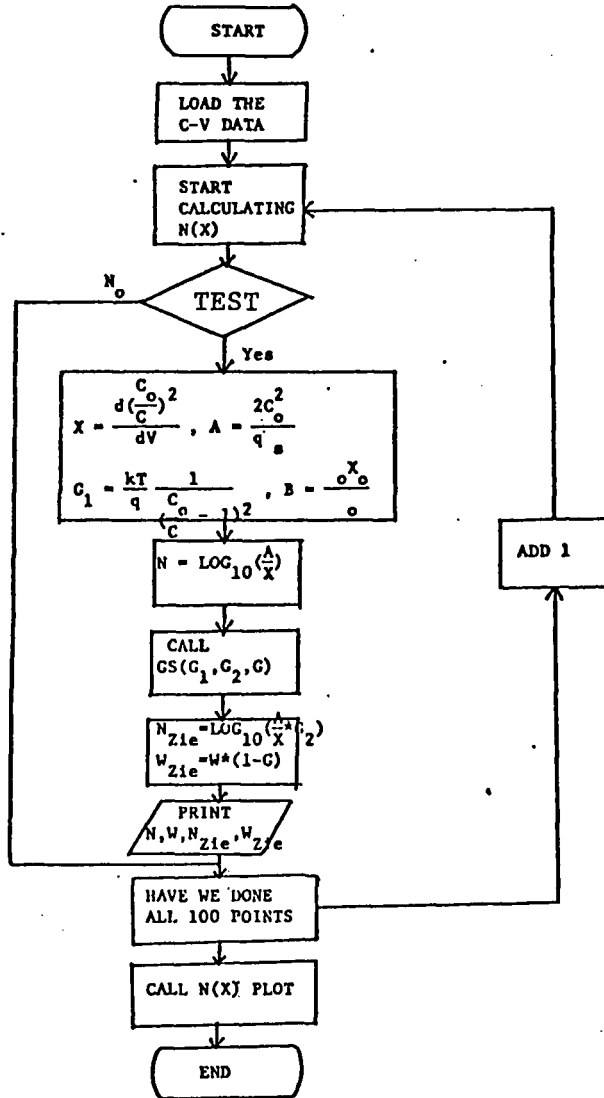


Figure 14. W/λ and g_1 vs. g_2 , of equation (A-27)
, (A-28) and (A-11). [2]

Appendix B-1-1

Flowchart for Calculating and Plotting N(X) with Ziegler's Correction from C-V Data



Appendix

```

10 *****
20 | THIS PROGRAM CALCULATES AND PLOTS N(X) WITH ZIEGLER'S
30 | CORRECTION FROM C-V DATA
40 |*****
50 DIM C(200),V(1000),Cn(1000),Ct(1000),W(1000),Cct(100),Cw(100),Cnt(100),Cn
(100),Ck(1000),Ccct(1000),Ccw(1000),Ccnt(1000),Ccnw(1000)
60 COM /G1/ G1
70 DJH Notes$(30),Gendate$(11),Doping_type$(1),Sample_code$(10),Data_file$(1
),File_specifier$(30),Answer$(1)
80 INTEGER High_volt,Points
90 REAL Bias_volt(1000),Capacitance(1000),Conductance(1000)
100 REAL Cap_const,Cond_const,Capac_oxide,Meas_freq
110 REAL Dev_area,V_source_bulk,Temperature
120 INPUT "ENTER DATA FILENAME:",Data_file$
130 INPUT "SPECIFY LEFT OR RIGHT HAND DRIVE",Answer$
140 IF Answer$="L" THEN
150 File_specifier$=Data_file$:INTERNAL,4,1"
160 ELSE
170 File_specifier$=Data_file$:INTERNAL,4,0"
180 END IF
190 |
200 | LOAD THE C-V DATA FILE
210 |
220 ASSIGN @Path1 TO File_specifier$:FORMAT OFF
230 ENTER @Path1;Notes$
240 ENTER @Path1;Gendate$,Doping_type$
250 ENTER @Path1;High_volt,Points
260 ENTER @Path1;Bias_volt(*),Capacitance(*),Conductance(*)
270 ENTER @Path1;Tempertaure
280 ASSIGN @Path1 TO *
290 FOR J=1 TO 1000 STEP 20
300 PRINT J,Bias_volt(J),Capacitance(J)
310 NEXT J
320 PRINT "ENTER COX"
330 INPUT Cox
340 |
350 | FLIP C-V DATA W.R.T. V
360 |
370 FOR J=1 TO 1000
380 V(1001-J)--Bias_volt(J)
390 Cn(1001-J)=Capacitance(J)/Cox
400 NEXT J
410 Q=1.6E-19
420 Aks=11.7
430 Eo=8.86E-14
440 Ako=3.9
450 Ak=8.62E-5*Q
460 T=300
470 Akt=Ak*T
480 Vt=Akt/Q
490 Xo=1.25E-5
500 Co=Ako*Eo/Xo
510 A=2*(Co+Cn)/(Q*Aks*Eo)
520 B=Aks*Xo/Ako
530 PRINT "ENTER JMAX"
540 INPUT Jmax
550 PRINT "ENTER JSTEP"
560 INPUT Jstep
570 |
580 | START CALCULATING N(X)

```

```

590 !
600 FOR J=99 TO Jmax STEP Jstep
610 IF (Cn(J+Jstep)-Cn(J-Jstep))<0 THEN GOTO 950
620 X=(1/(Cn(J+Jstep)*Cn(J+Jstep))-1/(Cn(J-Jstep)*Cn(J-Jstep)))/(V(J+Jstep)-
V(J-Jstep))
630 G1=Vt/((1/Cn(J)-1)*2)*X
640 Ca=A/X
650 !
660 ! N(X) WITHOUT CORRECTION
670 !
680 Ocnt(J)=LGT(A/X)
690 Ocnw(J)=B*(1/Cn(J)-1)*1.E+8
700 !
710 ! COMPARISON BETWEEN X AND 2*LD(LD2)
720 !
730 Ld2=2*SQR(2*Vt*Aks+En/(Q*Ca))*1.E+8
740 IF (Ocnw(J))>Ld2 THEN GOTO 930
750 PRINT J,X,Ocnw(J),Ld2
760 !
770 ! CALL CORRECTION TERMS
780 !
790 CALL Gs(G1,G2,G)
800 PRINT J,X,G1,G11,G2,G
810 IF (G2<-.33) THEN GOTO 900
820 !
830 ! N(X) WITH ZIEGLER'S CORRECTION
840 !
850 Ct(J)=A*G2/X
860 H(J)=B*(1/Cn(J)-1)*(1-G)
870 Occt(J)=LGT(Ct(J))
880 Ocw(J)=1.E+8*H(J)
890 GOTO 950
900 Ocw(J)=1.E+8*B*(1/Cn(J)-1)*(1-G)
910 Occt(J)=LGT(A*.33/X)
920 GOTO 950
930 Occt(J)=Ocnt(J)
940 Ocw(J)=Ocnw(J)
950 NEXT J
960 FOR J=499 TO Jmax STEP Jstep
970 PRINT J,Occt(J),Ocw(J),Ocnt(J),Ocnw(J)
980 NEXT J
990 !
1000 ! REDUCE DATA BY FACTOR JSTEP
1010 !
1020 FOR J=99 TO Jmax STEP Jstep
1030 Y=INT((J+1)/Jstep)
1040 Cct(Y)=Occt(J)
1050 Cw(Y)=Ocw(J)
1060 Cnt(Y)=Ocnt(J)
1070 Cnw(Y)=Ocnw(J)
1080 NEXT J
1090 FOR I=1 TO 100
1100 PRINT I,Cct(I),Cw(I),Cnt(I),Cnw(I)
1110 NEXT I
1120 !
1130 ! PLOT N(X) WITH AND WITHOUT CORRECTION
1140 !
1150 CALL Nvsx(0,1.E+4,Nb,300,Cct(*),Cw(*),100)
1160 CALL Nvsx(0,1.E+4,Nb,300,Cnt(*),Cnw(*),100)
1170 !
1180 ! SAVE N(X) DATA

```

```

1190 |
1200 PRINT "TYPE Y IF YOU WANT TO STORE THIS DATA"
1210 PRINT "TYPE N OTHERWISE"
1220 INPUT M$
1230 IF M$="N" THEN 1300
1240 PRINT "ENTER FILE NAME OF THE IMPURITY PROFILE"
1250 INPUT M$
1260 CREATE BDAT M$,1,3300
1270 ASSIGN @Path2 TO M$;FORMAT OFF
1280 OUTPUT @Path2;Cct(*),Cw(*),Cnt(*),Cnw(*)
1290 ASSIGN @Path2 TO *
1300 END
1310 !*****
1320 | SUBROUTINE FOR PLOTTING N(X) CURVE
1330 !*****
1340 SUB Nvsx(Xmin,Xmax,Nb,Temp,Concentration(*),Depth(*),Points)
1350 |
1360 | Plotting subroutine for N(X) CURVE
1370 |
1380 | Initialization
1390 DEG
1400 WINDOW Xmin-850,Xmax+200,13.5,18.5
1410 CSIZE 5,.4
1420 LORG 6
1430 |
1440 | Title of graph
1450 |
1460 MOVE (Xmax+Xmin)/2,18
1470 LABEL "CONCENTRATION .VS. DEPTH CURVE"
1480 |
1490 | Label axes
1500 |
1510 LORG 4
1520 MOVE (Xmax+Xmin)/2,13.5
1530 LABEL "DEPTH (1000 A)"
1540 LDIR 90
1550 LORG 6
1560 MOVE Xmin-750,16.5
1570 LABEL "LOG [CONCENTRATION (1/(CM^3))]"
1580 |
1590 | Number axes
1600 |
1610 LDIR 0
1620 CSIZE 2,.8
1630 LORG 6
1640 FOR I=Xmin TO Xmax STEP 1000
1650 MOVE I,14
1660 LABEL I/1000
1670 NEXT I
1680 |
1690 LORG 8
1700 FOR I=14 TO 18 STEP 1
1710 MOVE 0,I
1720 LABEL I
1730 NEXT I
1740 Lowx=9.E+39
1750 FOR I=1 TO Points
1760 IF Depth(I)<Lowx AND Depth(I)>0 THEN
1770 Lowx=Depth(I)
1780 END IF
1790 NEXT I

```



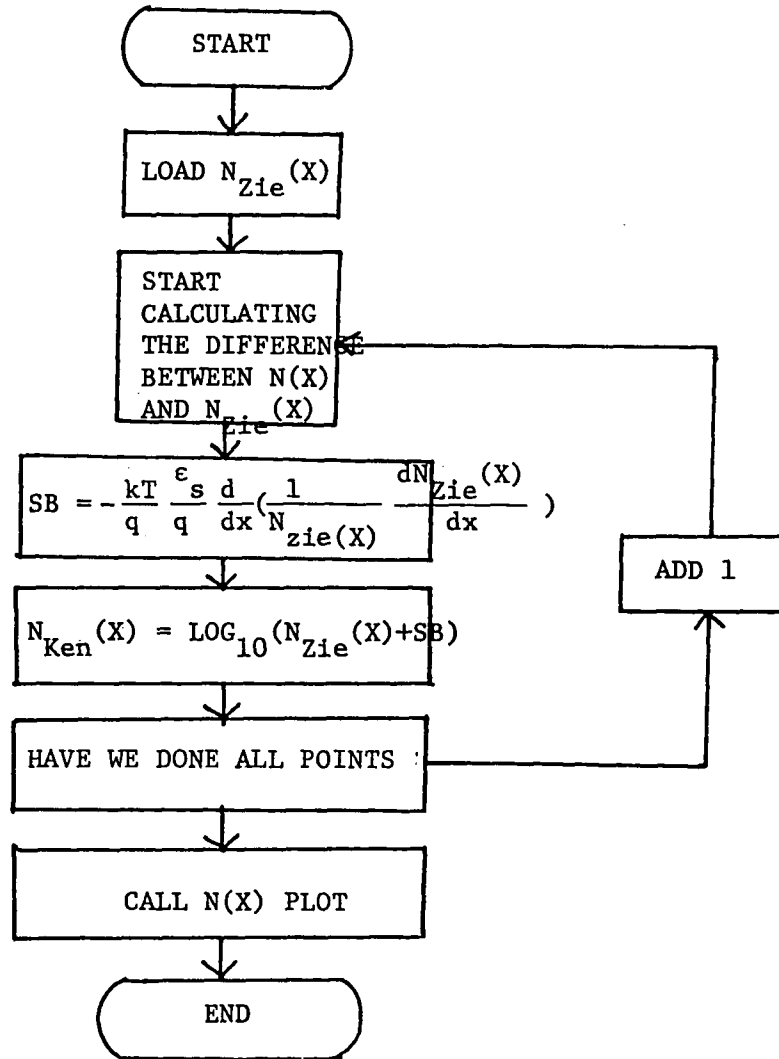
```

1800 !
1810 ! Draw axes and plot data points
1820 !
1830 AXES 1000,1,0,14,1,1
1840 CLIP Xmin,Xmax,13,18
1850 FOR I=1 TO Points
1860 IF Depth(I)=0 AND Concentration(I)=0 THEN GOTO 1880
1870 PLOT Depth(I),Concentration(I),+1
1880 NEXT I
1890 CLIP OFF
1900 SUBEND
1910 !*****
1920 ! SUBROUTINE FOR CALCULATING CORRECTION TERMS G1,G2 AND G
1930 !*****
1940 SUB Gs(G1,G2,G)
1950 COM /G1/ G1
1960 Dg=.001
1970 G=.001
1980 FOR I=1 TO 1000
1990 IF G=1 THEN GOTO 2180
2000 IF G<=0 THEN GOTO 2180
2010 !
2020 ! USE NEWTON-RAPHSON METHOD TO SOLVE G
2030 !
2040 F=(1-G)/(G-LOG(G)-1+.001)-2*G/(1-G)-G1
2050 Fp=(-1+1/G+LOG(G))/(G-LOG(G)-1+.001)2-2/((1-G)2)
2060 Newg=G-F/Fp
2070 IF ABS(G-Newg)<1.E-2 THEN GOTO 2090
2080 GOTO 2170
2090 G=Newg
2100 G1=G1
2110 IF G1>=.7 THEN GOTO 2190
2120 !
2130 ! CALCULATE G2
2140 !
2150 G2=ABS(G1/(2*G+(1-G)+G1))
2160 GOTO 2190
2170 G=G+Dg
2180 NEXT I
2190 SUBEND

```

Appendix B-2-1

Flowchart for Calculating and Plotting N(X) with Kennedy's Correction



Appendix B-2

```

10 !*****
20 ! THIS PROGRAM CALCULATES AND PLOTS N(X) WITH KENNEDY'S
30 ! CORRECTION NEAR THE JUNCTION
40 !*****
50 DIM Cct(200),Cw(200),Cnt(200),Cnw(200),A(100),Y(100),B(100),T(100),S(100)
60 REAL Beta(10)
70 !
80 ! LOAD N(X) DATA FILE
90 !
100 PRINT "ENTER FILE NAME OF THE IMPURITY PROFILE"
110 INPUT XS
120 ASSIGN @Path1 TO XS;FORMAT OFF
130 ENTER @Path1;Temp,Area,Vsb,Cct(*),Cw(*),Cnt(*),Cnw(*)
140 ASSIGN @Path1 TO *
150 !
160 ! ENTER PARATERS EXTRACTED FROM NON-LINEAR LEAST SQUARE METHOD
170 !
180 PRINT "ENTER # OF PARAMETERS"
190 INPUT K
200 PRINT "ENTER PARMETERS SEQUENTIALY"
210 FOR J=1 TO K
220 INPUT Beta(J)
230 NEXT J
240 Dx=.02
250 X=0
260 FOR I=1 TO 50
270 A(I)=X
280 Z1=Beta(1)*EXP(-Beta(2)*((X-Beta(3))^2))
290 Z2=Beta(4)*EXP(-Beta(5)*X)
300 Z3=Beta(6)
310 !
320 ! DEFINE FUNCTION FOR PLOT USE
330 !
340 Z=Z1+Z2-Z3
350 !
360 ! TAKE THE DIFFERENCE BETWEEN N(X) AND n(X)
370 !
380 Zx=(Z*(Z1/Beta(1)+(1-Beta(2)*((X-Beta(3))^2)))+(Beta(5)^2)*Z2)-(Beta(2)
X-Beta(3))*Z1+Beta(5)*Z2)*(Beta(2)*Z1+Beta(5)*Z2)/(Z^2)
390 Zc=(8.62E-5*1.6E-19*300*8.86E-14)/(1.6E-19)^2
400 Dz=Zc*Zx*1.E+8
410 Sa=-((2*Beta(2)*(X-Beta(3))+Z1+Beta(5)*Z2)/Z)^2+(Z1*(-2*Beta(2)+2*(B
a(2)^2)*((X-Beta(3))^2)+(Beta(5)^2)*Z2)/Z
420 Sh=-Zc+Sa*1.E+8
430 S(I)=LGT(ABS(Z+Sb))
440 T(I)=LGT(ABS(Z-Dz))
450 Y(I)=LGT(ABS(Z))
460 B(I)=A(I)*1.E+4
470 PRINT B(I),Y(I),S(I),Sb
480 X=X+Dx
490 NEXT I
500 PAUSE
510 !
520 ! PLOT N(X) CURVES WITH AND WITHOUT KENNEDY'S CORRECTION
530 !
540 CALL Nvsx(0,1.E+4,Nb,300,Cct(*),Cw(*),200)
550 CALL Nvsx(0,1.E+4,Nb,300,Cnt(*),Cnw(*),200)
560 CALL Nvsx(0,1.E+4,Nb,300,Y(*),B(*),50)
570 CALL Nvsx(0,1.E+4,Nb,300,S(*),B(*),50)
580 END
590 !*****

```

```

600 ! SUBROUTINE FOR PLOTTING N(X) CURVE
610 !*****
620 SUB Nvsx(Xmin,Xmax,Nb,Temp,Concentration(*),Depth(*),Points)
630 !
640 ! Plotting subroutine for N(X) CURVE
650 !
660 ! Initialization
670 DEG
680 WINDOW Xmin-850,Xmax+200,13.5,18.5
690 CSIZE 5,.4
700 LORG 6
710 !
720 ! Title of graph
730 !
740 MOVE (Xmax+Xmin)/2,18
750 LABEL "CONCENTRATION .VS. DEPTH CURVE"
760 !
770 ! Label axes
780 !
790 LORG 4
800 MOVE (Xmax+Xmin)/2,13.5
810 LABEL "DEPTH (1000 A)"
820 LDIR 90
830 LORG 6
840 MOVE Xmin-780,16.5
850 LABEL "LOG (CONCENTRATION (1/(CH*3)))"
860 !
870 ! Number axes
880 !
890 LDIR 0
900 CSIZE 2,.8
910 LORG 6
920 FOR I=Xmin TO Xmax STEP 1000
930 MOVE I,14
940 LABEL I/1000
950 NEXT I
960 !
970 LORG 8
980 FOR I=-14 TO 18 STEP 1
990 MOVE 0,I
1000 LABEL I
1010 NEXT I
1020 Lowx=9.E+39
1030 FOR I=1 TO Points
1040 IF Depth(I)<Lowx AND Depth(I)>0 THEN
1050 Lowx=Depth(I)
1060 END IF
1070 NEXT I
1080 !
1090 ! Draw axes and plot data points
1100 !
1110 AXES 1000,1,0,14,1,1
1120 CLIP Xmin,Xmax,13,18
1130 FOR I=1 TO Points
1140 IF Depth(I)=0 AND Concentration(I)=0 THEN GOTO 1160
1150 PLOT Depth(I),Concentration(I),+1
1160 NEXT I
1170 CLIP OFF
1180 SUBEND

```

APPENDIX C

*** STANFORD UNIVERSITY PROCESS ENGINEERING MODELS PROGRAM ***

*** VERSION 0-03 ***

```
1....TITL 3535 GATED DIODE SIMULATION
2....GRID DYSI=0.005, DPTH=0.6, YMAX=2.5
3....SUSS ORNT=100, ELEM=-, CONC=2.E14
4....PLOT TOTL=Y, CMIN=14, NOEC=4, WIND=2
5....PRINT TQTL=Y, HEAD=Y
6....COMM GROWING IMPLANT OXIDE
7....MODEL NAME=SPM1
8....STEP TYPE=DEPO, TIME=1, GRTE=0.076
9....COMM P-LAYER IMPLANT
10....STEP TYPE=IMPL, ELEM=0, DOSE=1.25E12, AKEV=40, MOUL=SPM1
11....PLOT TOTL=Y
12....STEP TYPE=DEPO, TIME=20, GRTE=0.05
13....STEP TYPE=OXID, TEMP=1050, TIME=30, MOUL=NIT0, MOUL=SPM1
14....COMM STRIPING OXIDE
15....STEP TYPE=ETCH, TEMP=25
16....COMM GROWING GATE OXIDE
17....STEP TYPE=OXID, TEMP=900, TIME=60, MOUL=WETG, MOUL=SPM1
18....STEP TYPE=OXID, TEMP=900, TIME=15, MOUL=NIT0, MOUL=SPM1
19....PLOT TOTL=Y
20....COMM POST-ANALING
21....STEP TYPE=OXIDE, TEMP=900, TIME=260, MOUL=NIT0, MOUL=SPM1
22....PLOT TOTL=Y
23....END
```

REFERENCES

1. D. P. Kennedy and R. R. O'Brien, *IBM J. Res. Dev.*, Vol. 13, P 212, 1971.
2. K. Ziegler, E. Klausmann, and S. Kar, *Solid-State Electron.*, Vol. 18, P189, 1975.
3. G. Lubberts and B. C. Burkey, *Solid-state Electron.*, Vol 22, P 47, 1979.
4. C. P. Wu, E. C. Douglas and C. W. Mueller, *IEEE. Trans Electron Devices* ED-22, P 319, 1975.
5. J. R. Brews, *J. App. Phys.* 44, P 3228, 1973.

VITA

Chen-Chung Chao was born on ~~January~~ January 5, 1956, to Mr. and Mrs. Tsun-Yun Chao. He received B.S. degree in Physics and M.S. degree in Applied Physics from National Tsing-Hua University, Hsin-Chu, Taiwan, in 1978 and 1980, respectively.

He is presently working towards the Ph.D. degree in Electrical and Computer Engineering at Lehigh Universty, Bethlehem, Pennsylvania.

His interests are in CMOS process technology and device modeling.